MOVING OBJECTS SEGMENTATION USING BOUNDARY LINKING AND BACKGROUND

Jun Ki Kim, Ho Suk Lee
Multimedia Laboratory, Dept. of Computer Engineering,
Hoseo University, Asan, Chungnam, South Korea

Keywords: Moving object edge, Moving object boundary, Boundary linking, Background, Moving object segmentation

Abstract: Moving object boundary is very important for moving object segmentation. We extract the moving object boundary from the moving object edge. But the object boundary shows broken boundary and we use a boundary linking to link the broken boundary. The boundary linking algorithm forms a quadrant around the terminating pixel in the broken boundary and searches forward other terminating pixel to link within a radius. The linking algorithm guarantees shortest distance linking. We register the background from image sequence. We construct two object masks, one from boundary linking and the other from the background, and use these two complementary object masks for moving object segmentation. We also filter out the moving cast shadow using gradient operator. The major characteristics of the proposed algorithms are accurate moving object segmentation, multiple moving objects segmentation, and the segmentation of an object which has holes in its region using these two object masks. We experiment the algorithms using the standard MPEG-4 test sequences and real video sequence. The proposed algorithms are very efficient and can process QCIF image more than 48 fps and CIF image more than 19 fps in a 2GHz Pentium-IV computer.

1 INTRODUCTION

The MPEG-4 video coding standard introduces the concept of Video Object Plane(VOP) to support content-based applications. The moving object segmentation has become an important research subject and has been receiving considerable amount of attention from many researchers for successful MPEG-4 content-based applications (Kim,2002)(Meier,1999)(Chien,2002)(Chien,2003).

One of the most important elements for moving object segmentation is to obtain moving object boundary. The object boundary, however, shows broken boundary caused by the edge detection failure due to instantaneous halt of the moving object. The object or the part of object often halts temporarily between consecutive frames and this causes the edge detection failure. Illumination variation and camera noise can also cause edge detection failure. The broken boundary makes it difficult to obtain an accurate moving object segmentation. The broken boundary should be supplemented with boundaries from other boundary sources and boundary linking and further using object mask. The other boundary sources include previous moving object edge, Canny edge of current frame, and background edge of current frame. The boundary linking is defined as the linking of two terminating pixels in the broken boundary. The boundary linking algorithm forms a quadrant around the terminating pixel and searches forward other terminating pixel to link in a clockwise concentric circle within a radius. The algorithm does not create a cycle and guarantees the shortest distance linking. The linking algorithm tries to link the broken boundary robustly within a search radius. But the linking algorithm does not try to link the broken boundary which is wider than the search radius, so for some images, there might remain broken boundaries after boundary linking. But for most images, we can obtain a completely linked moving object boundary after boundary linking. We use the object mask to deal with the case of wide broken boundary.

The main characteristics of the proposed algorithm are accurate moving object segmentation by boundary linking, the segmentation of an object which has holes in its region, and real-time performance. We use the standard MPEG-4 test sequences and a real video sequence for experiment. We assume that the camera and background are stationary.

The organization of paper is as follows. Section 2

Suk Lee H. and Ki Kim J. (2004).
MOVING OBJECTS SEGMENTATION USING BOUNDARY.
In *Proceedings of the First International Conference on E-Business and Telecommunication Networks*, pages 269-277
DOI: 10.5220/0001401302690277

gives the detailed introduction of the proposed moving object segmentation algorithms. Section 3 shows the experimental results of the algorithm and section 4 draws the conclusion.

2 MOVING OBJECT SEGMENTATION

2.1 Overall architecture

We consider the moving object segmentation as a process of development from initial moving object to final moving object segmentation. The initial moving object is actually the background change detection mask. We use the background change detection mask computed from the current frame and the registered background because it can yield more accurate moving object edge. The initial moving object is processed in two complementary ways. The two complementary ways are moving object boundary construction from moving object edge and boundary linking and noise elimination of initial moving object for object segmentation. The constructed object boundary, however, shows broken boundary so we try to link the broken boundary to obtain a completely linked boundary for most images. And finally we combine the results from two complementary object masks for accurate moving object segmentation and the segmentation of an object which has holes in its region. We use the connected component algorithm and morphological operation to eliminate the noise and to enhance the object mask boundary. Fig. 1 shows the overall system architecture.

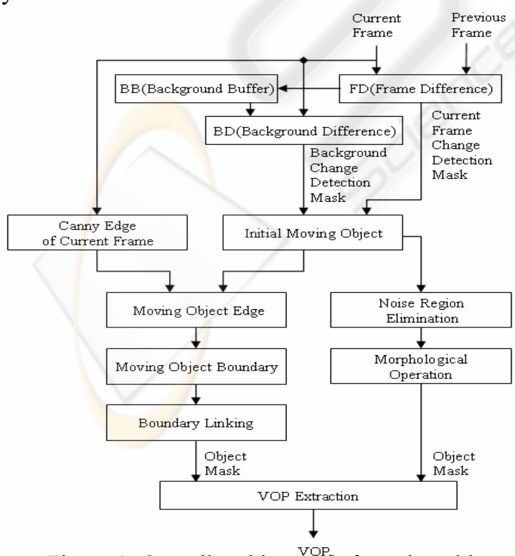

Figure 1: Overall architecture of moving object segmentation

FD means the pixel-based frame difference between the current frame and previous frame and generates the current frame change detection mask. BD means the frame difference between the current frame and background and generates the background change detection mask. BB means the background buffer which is used to register the background. The count value of FD frame difference is sent to BB to register the background. The moving object edge is constructed using the Canny edge of current frame and the initial moving object. We scan the constructed moving object edge horizontally and vertically and extract the moving object boundary. Then, we examine the object boundary and set the terminating pixels in the broken boundary regions and perform the space-oriented boundary linking robustly to obtain a completely linked moving object boundary. We construct the object mask of first type using this result. We also eliminate noise from the initial moving object and construct the object mask of second type. Then, we extract the VOP of the current frame using these two object masks.

2.2 Moving object edge construction

We construct the moving object edge as a process from initial moving object edge through intermediate and to final moving object edge. Fig. 2 shows the block diagram of the moving object edge construction.

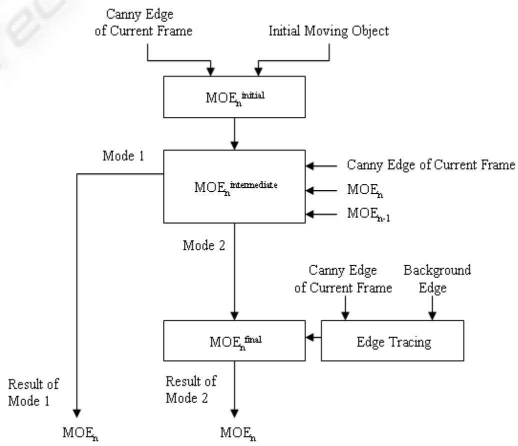

Figure 2: Moving object edge construction

The initial moving object edge is constructed using Canny edge (Canny, 1986) of current frame and the initial moving object. The intermediate moving object edge is constructed using Canny edge of current frame and the previous moving object edge to link the broken boundary region which is mostly caused by instantaneous halt of the object between the consecutive frames. After this process, the moving object edge construction is divided into two modes. In mode one, we regard the intermediate moving object edge as the final result. We can process the video sequences such as “Weather” and “Hall monitor” in mode one and can obtain a sufficient moving object edge for further processing. In mode two, we construct the final moving object edge using edge tracing. The edge tracing is implemented using Canny edge of current frame and background edge of current frame. We can process the “Claire” which does not have background and the “Akiyo” which has a high quality in mode two using edge tracing. The user can select the mode using a parameter.

2.2.1 Change detection and background

We use the absolute pixel difference as the test statistics for change detection. Under the hypothesis that there is no change in the current pixel, the pixel difference can be modeled using a zero-mean Gaussian distribution N(0, σ) with variance σ^2 (Aach,1993).

We register the background using stationary background filtering (Meier,1999). We use the background to generate the background change detection mask and it is used as the initial moving object.

2.2.2 Moving object edge

We define the edge as the pixels constituting the edge in the image. The following is the equation for initial moving object edge computation.

$$MOE_n^{initial} = \{e = e_1 \,\&\, e_2 \mid e_1 \in E_n^c,\ \ e_2 \in IMO\} \quad (1)$$

Here, E_n^c is the Canny edge of the current frame and *IMO* is the initial moving object. *e*, e_1, and e_2 are the edges. The operation & is the logical AND operation.

The intermediate moving object edge is as follows.

$$MOE_n^{intermediate} = \{e = e_1 \,\&\, e_2 \mid e_1 \in E_n^c,\ \ e_2 \in MOE_n \| \ e_2 \in MOE_{n-1}\} \quad (2)$$

Here, MOE_n is the current moving object edge and MOE_{n-1} is the previous moving object edge. The || operation means the logical OR operation. It means the union of the edges of MOE_n with the edges of MOE_{n-1} to link the broken boundaries in MOE_n , caused by the instantaneous halt of the object. The final moving object edge is computed as follows.

$$MOE_n^{final} = \{e = e_1 \| e_2 \mid \ \ e_1 \in MOE_n^{intermediate},\ e_2 \in E_n^c \,\&\, e_2 \notin E_n^b\} \quad (3)$$

Here, E_n^b is the background edge. The logical OR operation means the union of the edges of Canny edge of current frame excluding background edges with the intermediate moving object edges in order to obtain the more linked final moving object edge. We call this edge tracing. We find edge tracing quite effective when the background has no noise or when the image has a high quality such as the “Akiyo” or the “Claire”. We can see the edge tracing results in Fig. 4 (c1) through (c4).

2.2.3 Edge tracing

Edge tracing is performed in mode two of moving object edge construction. Edge tracing uses Canny edge of current frame E_n^c and the background edge of current frame E_n^b . The followings are edge tracing steps.

(step1) Construct the background edge E_n^b *(x,y)* using the following equation automatically.

$$E_n^b(x, y) = E_n^c(x, y) - MOE_n^{intermedia} \quad (4)$$

But the background edge contains some still remaining uneliminated object pixels as shown Fig. 3 (a). We use the connected component algorithm to eliminate these remaining object pixels in the background edge and obtain a clear background edge as shown in Fig. 3 (b).

(step2) Scan $MOE_n^{intermediate}(x,\ y)$ by horizontal scanline and locate the first pixel encountered.

(step3) Search around the neighboring pixels of the pixel found in **(step2)** in 8-connected way to start the edge tracing in $MOE_n^{intermediate}$.

(step4) Check the presence of a pixel in E_n^c *(x,y)* at the corresponding coordinate position during edge tracing in $MOE_n^{intermediate}$ until the edge tracing comes to the terminating pixel in $MOE_n^{intermediate}(x,y)$. If there exists a pixel at the corresponding coordinate, perform edge tracing along the E_n^c *(x,y)* edge as long as the pixel of E_n^c *(x,y)* under edge tracing does not encounter the background edge $E_n^b(x,y)$ constructed in **(step1)**. And include the traced edge of E_n^c *(x,y)* into MOE_n^{final}. If it encounters the background edge, edge tracing stops.

(step5) Return to **(step2)** and continue.

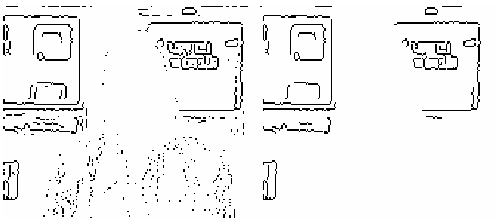

(a) (b)

Figure 3: Background edge (Akiyo 11th)
(a) Background edge with remaining object pixels,
(b) Background edge with no object pixels

Figure 4 shows the moving object edge construction results.

(a1) $MOE^{intermediate}$ (a2) $MOE^{intermediate}$

(a) Hall monitor 45th

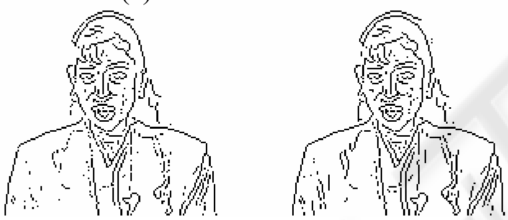

(b1) $MOE^{intermediate}$ (b2) $MOE^{intermediate}$

(b) Akiyo 29th

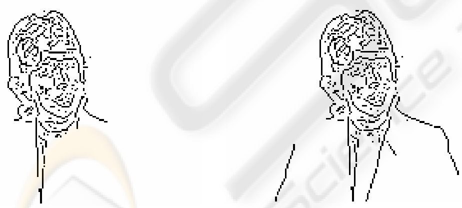

(c1) $MOE^{initial}$ 90th (c2) $MOE^{intermediate}$ 90th

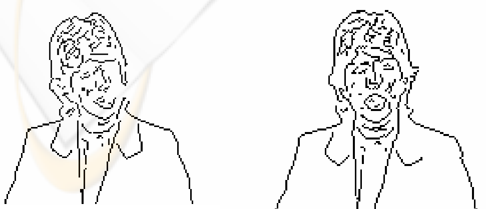

(c3) MOE^{final} 90th (c4) MOE^{final} 17th

Figure 4: Moving object edge
(a) Hall monitor, (b) Akiyo, (c) Claire

Fig. 4 shows the moving object edge of (a) "Hall monitor", (b) "Akiyo", and (c) "Claire". The left column of (a) and (b) were produced using the current frame change detection mask as in (Kim,2002) and the right column of (a) and (b) using the background change detection mask. We can see the more accurate moving object edge in the right column. For (a) and (b), we use the intermediate moving object edge as the final result. The (c) "Claire" shows the process of moving object edge construction using edge tracing. Fig. 4 (c4) was shown for more demonstration.

2.3 Moving object boundary

2.3.1 Moving object boundary extraction

First, we eliminate small isolated noise pixels from the moving object edge. Then, we scan the moving object edge by horizontal and vertical scanline and obtain the moving object boundary. The following Fig. 5 shows the moving object boundary of "Claire".

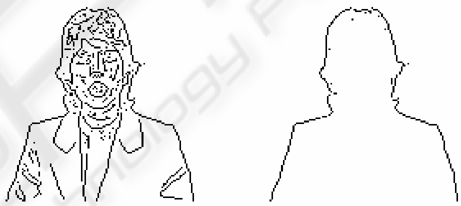

(a) (b)

Figure 5: Moving object boundary
(a) Moving object edge, (b) Moving object boundary

2.3.2 Moving object boundary linking

We examine the moving object boundary image and set terminating pixels at the final end pixels of the broken boundary line. Fig. 6 (a1) and (a2) show the "Hall monitor" with terminating pixels, (b) shows the "Akiyo" with terminating pixels, and (c) shows the "Claire" with terminating pixels. The actual terminating pixel is just a single pixel but we enlarge it for clear vision.

(a1) Hall monitor 54th (a2) Hall monitor 69th
(a) Hall monitor

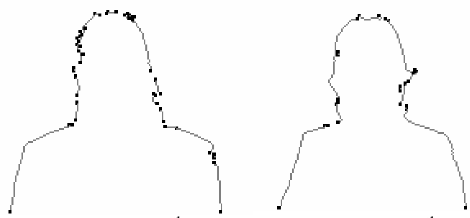

(b) Akiyo 18th (c) Claire 11th

Figure 6: Terminating pixel setting
(a) Hall monitor, (b) Akiyo, (c) Claire

Various edge linking algorithms considering the pixel gradient magnitude are explained using examples (Gonzalez,2002). An edge linking algorithm considering three types of break points using window is explained in (Hajjar,1999). The proposed boundary linking algorithm is a space-oriented geometric algorithm. The boundary linking algorithm links the broken boundary by inserting pixels from one terminating pixel to the other terminating pixel. The algorithm considers the linking direction first. The algorithm forms a quadrant around the terminating pixel and searches forward other terminating pixel to link within a radius in concentric circle. The algorithm always guarantees shortest distance linking and does not create a cycle. We see that the boundary linking algorithm forms the object boundary in the broken boundary region accurately because the terminating pixels used for boundary linking in the broken boundary region exist on the object boundary.

We give a more detailed explanation. We assume a virtual pixel around the terminating pixel. The virtual pixel is assumed in the forward direction of the terminating pixel by considering the slope of the terminating pixel. The purpose of virtual pixel is to predetermine the general direction toward which the broken boundary is going to be linked from the terminating pixel.

However, it is usually seldom the case that every terminating pixel ought to be linked only in the direction of the virtual pixel, because the pixel distribution varies significantly according to the characteristics of the input image. Thus, we form a quadrant for a more general search range around the terminating pixel $T_0 = (0,0)$ in the direction of the virtual pixel $V_0 = (V_x, V_y)$. The algorithm begins by positioning the terminating pixel at the coordinate origin. The boundary linking operation is now carried out within the quadrant from the terminating pixel. First, we compute the angle between the terminating pixel and the virtual pixel. If we let θ_v as the angle between T_0 and V_0 we compute

$$\theta_v = \cos^{-1} \frac{V_x}{\sqrt{V_x^2 + V_y^2}} * \pi / 180 \tag{5}$$

and we search another terminating pixel T_1 to link around the terminating pixel T_0 within the quadrant in clockwise concentric circle within a given radius. Now, if we find another terminating pixel $T_1 = (T_x, T_y)$ around the current terminating pixel T_0. We compute the angle θ_s between T_0 and T_1.

$$\theta_s = \cos^{-1} \frac{T_x}{\sqrt{T_x^2 + T_y^2}} * \pi / 180 \tag{6}$$

Then the condition and operation of boundary linking can be summarized as follows.

procedure boundary_linking( )
{
if $(2\pi + \theta_v - \frac{\pi}{4} \le \theta_s \le 2\pi + \theta_v + \frac{\pi}{4})$
then {
link $T_0 = (0,0)$ to $T_1 = (T_x, T_y)$
} else expand the quadrant to half plane
and perform boundary linking from
$T_0 = (0,0)$
}

If the angle θ_s of the terminating pixel T_1 is within the range as computed above, the boundary linking is carried out from the terminating pixel T_0 to the terminating pixel T_1. If the angle θ_s is not within the range, we expand the quadrant to half plane and perform the boundary linking iteratively from $T_0 = (0,0)$.

We find other terminating pixel to link within the radius around the starting terminating pixel within 5 iterations most of the time in the experiment. In other cases, the boundary linking algorithm searches the pixel in the expanded half plane. We continue boundary linking until there remain no more terminating pixels to link. Fig. 7 shows the constructed moving object boundary of Fig. 6 after boundary linking.

The linking algorithm tries to link the broken boundary robustly within a search radius which is determined experimentally. The linking algorithm does not try to link the terminating pixel which is located farther than the search radius, because it can link the wrong terminating pixel in trying to do so. For example, the search radius for “Hall monitor” is set at 8 and “Akiyo” at 12.

The algorithm sets 20 terminating pixels in Fig. 6 (a1) and performed 11 boundary linking in Fig. 7 (a1) “Hall monitor”. In Fig. 6 (b) “Akiyo” 18th, the algorithm sets 39 terminating pixels and performed 18 boundary linking. We can see several broken boundaries in Fig. 6 (a1), (a2), (b), and (c) and can see their corresponding completely linked object boundary in Fig. 7 (a1), (a2), (b), and (c) respectively. Currently, we can see two object boundaries in some boundary, one by moving object edge itself, and the other by boundary linking, but these seemingly double boundaries do not cause a problem, because we map the object texture to the outermost boundary.

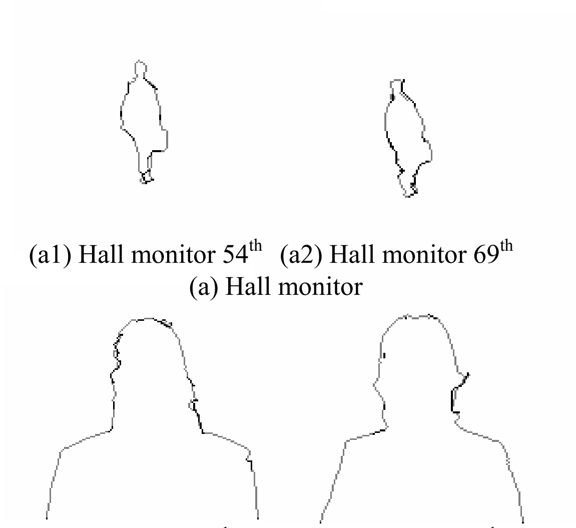

(a1) Hall monitor 54th (a2) Hall monitor 69th
(a) Hall monitor

(b) Akiyo 18th (c) Claire 11th

Figure 7: Moving object boundary linking
(a) Hall monitor, (b) Akiyo, (c) Claire

2.3.3 Moving object linking at the bottom

We construct the moving object boundary as shown in Fig. 7. But the moving object shows boundary disconnection at the bottom. Fig. 8 (a) and (b) show the connected moving object boundary of Fig. 7 (b) and (c).

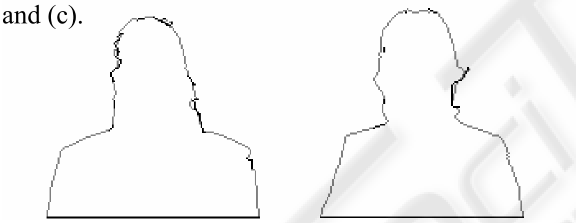

(a) Akiyo 18th (b) Claire 11th

Figure 8: Object boundary connection at the bottom
(a) Akiyo, (b) Claire

2.4 Video object plane extraction

We perform moving object extraction with two object masks. We use the object mask made from boundary linking and the object mask from initial moving object. We call the former the object mask of first type and the latter the object mask of second type. The advantage of the first type is the accurate moving object boundary. But it cannot handle the case of an unlinked broken boundary which could exist in the wide broken boundary and the segmentation of an object which has holes in its region. The second type can handle these situations but the boundary it shows is somewhat coarse. Therefore, we use these two object masks in combination.

2.4.1 Using the object mask of first type

Fig. 9 shows moving object extraction using the object mask of first type. Fig. 9 (a) is the moving object mask and (b) is the object segmentation result. Fig. 9 (b) shows an accurate object boundary

(a) (b)

Figure 9: Object extraction with first mask (Akiyo)
(a) Moving object mask, (b) Segmentation result

2.4.2 Using the object mask of second type

Fig. 10 shows the block diagram of the second type object mask construction.

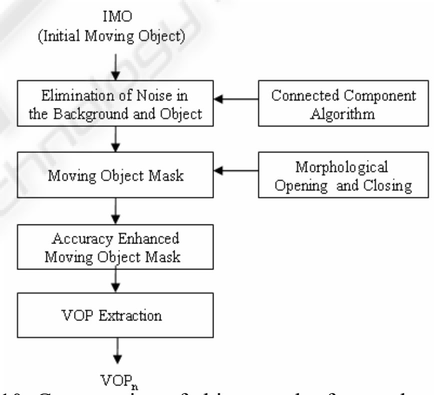

Figure 10: Construction of object mask of second type

We show in Fig. 11 the moving object extraction using the object mask of second type. Fig. 11 (a) shows the initial moving object with noise, (b) shows the object mask of second type with clear background and object images, and (c) shows the object segmentation result.

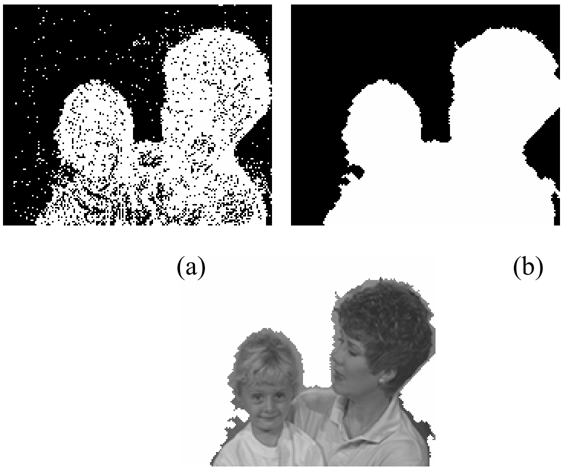

(a) (b)

(c)

Figure 11: Moving object extraction 45th
(a) Initial moving object, (b) Object mask of second type,
(c) Segmentation result

Fig. 12 shows moving object extraction result of "Akiyo" using the object mask of second type. The "Akiyo" object shows somewhat coarse object boundary.

(a) (b)

Fig. 12 Object extraction with second mask (Akiyo)
(a) Moving object mask, (b) Segmentation result

2.4.3 Using both object masks

Following is an expression for moving object extraction using both object masks.

$$Moving\_object_n(x,y) = \begin{cases} Current\_frame_n(x,y) & if \quad mask\_first_n(x,y)=1 \\ & \quad \& \quad mask\_second_n(x,y)=1 \\ 0 & otherwise \end{cases} \tag{7}$$

Moving_object$_n$(x,y) means the extracted moving object. The *mask_first$_n$(x,y)* means the object mask of first type and *mask_second$_n$(x,y)* the object mask of second type. The *&* is the logical AND operation. The moving object is extracted from the current frame if and only if both object masks are equal to 1. Thus we can handle wide broken boundaries and can segment the object which has holes using the object mask of second type. Fig. 13 (a) shows "Mother&Daughter" which has a wide broken boundary and (b) shows the segmentation result using expression (7). Fig. 13 (c) and (d) show the segmentation of "Junki" real video which has holes in its region using expression (7), too.

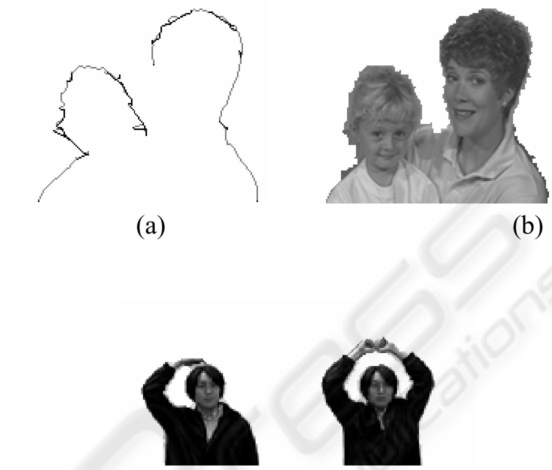

(a) (b)

(c) (d)

Figure 13: Moving object extraction with both masks
(a) Mother&Daughter with a wide broken boundary,
(b) Mother&Daughter segmentation result,
(c) Junki real video A, (d) Junki real video B

2.4.4 Moving cast shadow filtering

The moving cast shadow is composed of a dark region called umbra and a soft transition region called penumbra (Stauder,1999). We apply the Roberts gradient operator to filter out the moving cast shadow. This shadow filtering operation can be executed to the input image.

3 EXPERIMENT

We experiment the moving object segmentation algorithm using the MPEG-4 standard test image sequences such as "Hall monitor", "Claire", "Akiyo", "Weather" and "Junki" real video.

3.1 Objective evaluation

We use the error percentage measure (Chien,2002) for the objective evaluation. The error percentage measures the cumulative error between the original image and the segmented image.

$$Error\_Percentage = \frac{\sum_W \sum_H (a(x,y) \oplus OM(x,y))}{W \times H} \times 100\% \tag{8}$$

The *a(x, y)* is the alpha map of the original image used for reference. ⊕ is the Exclusive-OR operation. The *OM(x, y)* is the alpha map of the segmented image. *W* is the width and *H* is the height. Fig. 14 shows the error percentage graph for "Claire", "Akiyo", and "Weather".

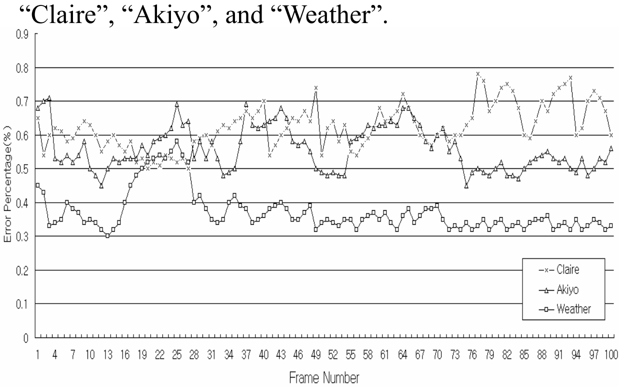

Figure 14: Error percentage graph

The size of image sequence is CIF(352x288) and it is input 25 frames/sec. We obtained the *a(x, y)* reference image sequence by segmenting it manually using the PHOTOSHOP tool in order to obtain the accurate reference image. Also, we obtained the *OM(x, y)* by applying the proposed object segmentation algorithm.

If there is no difference, the error percentage is 0%. If the error percentage is above 1.5%, then the segmented moving object could show some visually recognizable difference from the input moving object.

The error percentage values we obtained from our experiments are less than 0.78% for these image sequences. This value indicates that the segmented moving object by our algorithm is visually very similar to the manually segmented moving object frames from the input image sequence and validates that the proposed segmentation algorithm can segment the objects very accurately. In Fig. 14, frames 3 and 4 of "Akiyo" and "Weather" show some high value of error percentage and frame 49, 79, and 94 of "Claire" show high value of error percentage because the object moves somewhat faster in these frames.

We can compare Fig. 14 with Fig. 7 of (Chien,2002) and can see that the error percentage results of "Akiyo" and "Weather" of our approach are comparable with those results.

Table 1 shows the performance statistics of our algorithm and other approaches for comparison. We use the P-IV CPU with 2.0GHz as the experiment CPU. We have optimized the implementation of computation intensive algorithms to satisfy the real-time requirement of various multimedia applications.

Table 1: Performance statistics

Algorithm	Test CPU	Sequence	Frames	Total processing time (msec)	Frames/second
Proposed	P-IV 2.0G	Hall Monitor(CIF)	298	15691	19.02
		Hall Monitor(QCIF)	328	4541	72.25
		Akiyo(CIF)	298	15397	19.38
		Akiyo(QCIF)	298	5030	59.25
		Claire(QCIF)	492	7002	70.27
		Mother&Daughter(QCIF)	298	6107	48.83
		Weather(360x243)	298	12844	23.22
Changick Kim(2002)	P-II 450M			(about 0.4 sec/frame)	
Shao-Yi Chien(2002)	P-III 450M	CIF type			10
		QCIF type			25
Shao-Yi Chien(2003)	P-III 800M	QCIF type		(106.64 msec/frame)	9.4

Table 1 shows the performance statistics. The table shows the test sequences, total frames, total processing time, and frames per second. The test sequences are CIF(352x288) and QCIF(176x144) standard MPEG-4 test sequences such as "Hall monitor", "Akiyo", "Claire", "Mother&Daughter", and "Weather". For example, the proposed system can process 72.25 frames per second for "Hall monitor" QCIF sequence, in other words, the system spends 0.0138 second per frame for "Hall monitor" QCIF sequence. We have included the performance results of (Kim,2002),(Chien,2002), and (Chien,2003) in the table for comparison. The approach (Chien,2002) can process QCIF at 25 fps and CIF at 10 fps using P-III 450MHz CPU. The approach (Chien,2003) can process QCIF at 9.4 fps using P-III 800MHz. The test CPUs are different but we can conclude that the proposed algorithms are more efficient than those algorithms.

3.2 Subjective evaluation

We show the moving object segmentation results of "Hall monitor", "Weather(360x243)" in Fig. 15. We also use "Junki" real video sequence to demonstrate the segmentation of an object which has holes in its region.

(a1) Hall monitor 45th

(a2) Hall monitor 152th and 219th

(a) Hall monitor

(b)Weather 217th

(c) Junki real video 158th

Figure 15: Moving object segmentation

(a) Hall monitor, (b) Weather, (c) Junki real video

We see that our algorithm can produce the accurate moving object segmentation and can segment the multiple moving objects and the object which has holes in its region using these two complementary object masks. We can see a small hole in the upper part of Fig. 15 (b) between the hair and forehead and also can see two holes in (c) clearly.

We can compare these segmentation results with the results in (Kim,2002),(Meier,1999),(Chien,2002), and (Chien,2003). Our segmentation results are better than those results in terms of the accuracy of the segmentation result because we use the object boundary linking for accuracy. The proposed segmentation algorithm can segment an object which has holes in its region as shown in (b) and (c) in Fig. 15. But none of references demonstrate this. Particularly, we can see in (d) and (e) of Fig. 9 of (Chien,2002) that the approach does not segment the object which has a hole in its region. We can also compare our "Mother&Daughter" segmentation results of Fig. 13 (b) with those of Fig. 16 and Fig. 17 of (Chien,2003) and we can see that our results are better.

4 CONCLUSION

We propose a novel moving object edge construction algorithm, a space-oriented geometric boundary linking algorithm, and a segmentation algorithm using two object masks. We can achieve more accurate moving object segmentation, multiple moving objects segmentation, and the segmentation of an object which has holes in its region using these algorithms.

We have shown the performance of our proposed algorithms using standard MPEG-4 test image sequence and a real video from camera. The proposed algorithms are very efficient and can process QCIF image more than 48 fps and CIF image more than 19 fps in a personal computer for real-time content-based applications.

REFERENCES

Kim, Changick, Hwang, Jenq-Neng, "Fast and Automatic Video Object Segmentation and Tracking for Content-Based Applications," IEEE Trans. on Circuits and Systems for Video Technology, Vol. 12, No. 2, pp.122-129, Feb. 2002.

Meier, Thomas, Ngan, King N., "Video Segmentation for Content-Based Coding," IEEE Trans. on Circuits and Systems for Video Technology, Vol. 9, No. 8, pp.1190-1203, Dec. 1999.

Chien, Shao-Yi, Ma, Shyh-Yih, Chen, Liang-Gee, "Efficient Moving Object Segmentation Algorithm Using Background Registration Technique," IEEE Trans. on Circuits and Systems for Video Technology, Vol. 12, No. 7, pp.577-586, July 2002.

Chien, Shao-Yi, Huang, Yu-Wen, Chen, Liang-Gee, "Predictive Watershed : A Fast Watershed Algorithm for Video Segmentation," IEEE Trans. on Circuits and Systems for Video Technology, Vol. 13, No. 5, pp.453-461, May 2003.

Canny, John, "A computational approach to edge detection," IEEE Trans. on Pattern Analysis and Machine Intelligence, Vol. 8, No. 6, pp. 679-698, Nov. 1986.

Aach, T., Kaup, A., Mester, R., "Statistical model-based change detection in moving video," Signal Processing, Vol. 31, pp. 165-180, March 1993.

Stauder, Jürgen, Mech, Roland, Ostermann, Jörn, "Detection of Moving Cast Shadows," IEEE Trans. on Multimedia, Vol. 1, No. 1, pp. 65-76, March 1999.

Gonzalez, Rafael C., Woods Richard E., Digital Image Processing, Prentice-Hall, Inc., 2002.

Hajjar, Amjad, Chen, Tom, "A VLSI Architecture for Real-Time Edge Linking," IEEE Trans. on Pattern Analysis and Machine Intelligence, Vol. 21, No. 1, pp. 89-94, Jan. 1999.